EXIT TIMES AND TRANSPORT FOR SYMPLECTIC TWIST MAPS

R.W. Easton, J.D. Meiss and S.Carver
Program in Applied Mathematics
University of Colorado
Boulder, CO 80309-0526

November 3, 1992

Abstract

The exit time decomposition of a set yields a description of the transport through the set as well as a visualization of the invariant structures inside it. We construct several sets, based on the ordering properties for orbits of twist maps, that are computationally easier to deal with than the construction of resonances. Furthermore these sets can be constructed for four and higher dimensional twist mappings. For the four dimensional case—using the example of Froeshlé—we find "practically" invariant volumes surrounding elliptic fixed points. The boundaries of these regions are remarkably sharp, and apart from some "holes", the regions appear to be connected.

1. Introduction

An understanding of transport phenomena in symplectic mappings is of importance in many applications including plasma confinement, particle accelerators, chemical reaction dynamics, and fluid mixing [1-3]. Indeed, the Poincaré mapping for any Hamiltonian system is symplectic, and Hamiltonian descriptions are fundamental for most physical systems.

The primary goal of a transport theory is to characterize the rates at which phase space volume moves from one region to another. Often the regions of interest are dictated by the application—for example in a particle accelerator the phase space domain corresponding to a well collimated, low temperature beam—or one may choose the regions to study the transition between qualitatively different kinds of motion.

Understanding transport is a first step in the statistical analysis of dynamical systems. If a system has simple statistical properties, then it could be treated using ergodic theory. Such systems include Anosov systems, Bernoulli systems, and the like. For example, a measure preserving transformation f of a finite measure space with measure μ is said to be *mixing* if given any two measurable sets A and B, $\mu(f^n(A)\cap B) \to \mu(A)\mu(B)$ as $n\to\infty$. Unfortunately such ideal properties are rarely found in physically motivated maps.

For the case of two dimensional maps, the description of transport in terms of turnstiles [4], resonances [5,6] and lobes[7] is well developed and efficient. The turnstile picture gives good predictions as to the scaling of transport near its onset, and describes the most effective barriers to transport (the cantori). The resonances give a complete partition of phase space into dynamically distinct behaviors [5,8]. A complete description of transport can be given in terms of the iteratesof the lobes of the turnstiles of these resonances; unfortunately, the lobe dynamics approach does not provide insight into transport rates, nor in to the fundamental question of the existence of algebraic decays. Simple approximate descriptions of this transport process, in terms of a Markovian description, while yielding easily computable predictions, give only a qualitative and difficult to justify description of the transport (including an explanation for algebraic decay [9])except in special cases where they are quantitatively accurate [10].

For symplectic maps of four or more dimensions, it is difficult to obtain a description of transport in terms of escape through turnstiles, except in the special case of a two dimensional map with a turnstile that is weakly coupled to an integrable two dimensional map[11]. Otherwise, for fully coupled 4d mappings, there has not been a construction of turnstiles or resonances.

Nonetheless, as we will show below, it is quite clear computationally that structures analogous to resonances exist in these systems. In fact onewould like to develop a notion of "practical stability"—orbits are trapped in a region of phase space for all practical purposes even if, as one believes, many will eventually escape by the Arnol'd mechanism (Arnol'd diffusion). Practical stability would extend thetheory of Nekhoroshev [12], which guarantees that the actions of an integrable Hamiltonian perturbed by $O(\varepsilon)$ will drift only by $O(\varepsilon)$ in exponentially long times (these ideas are exploited in the work of[13]). Our concern is not this case of weak perturbation, but that of fully coupled systems.

In this paper we develop several new statistical measures describing transport. These are based on the exit time decomposition of a set[6], which we review in §2. The sets we consider are tailored to probing the orbits trapped in the neighborhood of an elliptic periodic orbit.

For the case of twist maps, the Lagrangian description of the dynamics leads to the notion that orbits trapped near an elliptic (minimax) orbit must live in the orbit of the gaps formed by its hyperbolic (minimizing)partner. We discuss the exit time decomposition the set based on these gaps in §5 and prove that the set of orbits trapped forever in the strips is identical to those orbits trapped in the resonance. We also introduce the concept of the width of an orbit in§6, which is easier to compute than the escape from the orbit of gaps since the hyperbolic orbit need not be computed. The set of orbits with width less than one is also identical to the invariant set of the resonance.

Generalizations of these concepts to higher dimensions are discussed in §7.

2. Exit Times

A typical question one would like to answer is illustrated by the case of a periodically driven frictionless pendulum. Suppose the pendulum is initially swinging back and forth. What is the probability that n periods later it will be rotating? There is a region in phase space that corresponds to rocking motion. The fraction of initial states that exit this region in exactly n periods is the desired probability. In order to discuss questions like these, we introduce several measures of escape times.

Let f be a mapping on some phase space, and A and B be sets in this space. As a basis for our statistical measures we focus attention on the minimum time for points of A to reach B. Define a *crossing time function* t: $A \to [0,\infty]$ by

$$t(a) = \begin{cases} \infty \text{ if } f^n(a) \notin B \text{ for all } n > 0 \\ \text{the least } n \text{ such that } f^n(a) \in B \text{ otherwise} \end{cases} \tag{1}$$

If B is the complement of A then the crossing time function is called the *exit time* and denoted t^+. If the map f is invertible, we define the *backward exit time* for a point $a \in A$ as

$$t^-(a) = \begin{cases} \infty \text{ if } f^{-n}(a) \in A \text{ for all } n > 0 \\ \text{the least } n \text{ such that } f^{-n}(a) \notin A \text{ otherwise} \end{cases} \tag{2}$$

The *transit time* for a point in A is the sum of the forward and backward exit times for that point.

The subset of points in A that exit in time j is denoted $\mathcal{E}_j$, those that have backward exit time j are denoted $\mathcal{I}_j$ (for *incoming)*, and those with transit time j are denoted $\mathcal{T}_j$. The *exit set* for A is the set $\mathcal{E} \equiv \mathcal{E}_1$,and the *entry set* is $\mathcal{I} = \mathcal{I}_1$. If the set A is measurable then so are various sets defined by the exit time functions.

The *survival sequence* associated with A is the sequence$\{s_j\}$ where s_j is the measure of the set of points in A that exit in time greater than or equal to j. The *escape time distribution*, $e_j \equiv s_{j+1} - s_j$, is the measure of particles that escape at time j.

3. Twist Maps

For our purposes a *twist map* is an exact symplectic map†

$$(x', y') = f(x,y) \tag{3}$$

on $T^d \times R^d$, such that the map φ: $(x,y) \to (x,x'(x,y))$ is a diffeomorphism [14,15] It is sufficient that the matrix _x′/_y be nonsingular, and we will require this to be the case. We denote an orbit by the sequence $(x_t, y_t) = f(x_{t-1}, y_{t-1})$.

A twist map can written in a Lagrangian form Λ: $(x_{t-1}, x_t) \to (x_t, x_{t+1})$, and an orbit of such a map is determined by a sequence $\{\ldots x_t, x_{t+1}, \ldots\ldots\}$. Often we will consider a lift of the map in order to distinguish between orbits that rotate and those that do not, so that the configuration $x \in R^d$, rather than T^d.

An important property of orbits of a twist map is the *frequency vector* , $\omega \in R^d$, defined as the limit

$$\omega = \lim_{t \to \infty} \frac{x_t}{t} \tag{4}$$

† A mapping is exact symplectic if the integral of y dx over an arbitraryclosed loop is invariant upon iteration.

if it exists. In particular, a periodic orbit is defined by the condition $x_{t+n} = x_t + m$, so it has a rational frequency $\omega = m/n$, where $m \in Z^d$, and n is the minimal period of the orbit.

The standard example of a twist mapping is

$$f: \begin{cases} y \to y - \nabla v(x) \\ x \to x + y - \nabla v(x) \end{cases} \tag{5}$$

where the potential v(x) is periodic, $v(x+m) = v(x)$ for $m \in Z^d$. The map can be expressed in Lagrangian form as

$$\Lambda: \begin{cases} x \to x' \\ x' \to 2x' - x - \nabla v(x') \end{cases} \tag{6}$$

For the two dimensional case, (5) becomes the "standard map" upon the choice

$$v(x) = -\frac{k}{4\pi^2}\cos(2\pi x) \tag{7}$$

For all k>0 this map has hyperbolic fixed points *p* and *q* located at (-.5,0) and (.5, 0). These points are connected by heteroclinic orbits going from the first to the second and from the second back to the first forming a heteroclinic cycle. There is an elliptic fixed point located at (0,0) for 0<k<4. This orbit becomes reflection hyperbolic for larger values of k.

We will also study a four dimensional example of (5) in §7.

4. Resonance Zones

One way in which orbits can be grouped into sets with similar properties is in terms of resonances: a *resonance zone* for a hyperbolic periodic orbit is a region of phase space within which orbits have motion "similar" to that of the periodic orbit. The boundary of the resonance is constructed from initial segments of stable and unstable manifold of the hyperbolic orbit; an *initial segment* of stable manifold is a segment from the periodic point to some end point, e.g. from the point *q* to the point *a* in fig. 1. A *resonance zone* is a compact region bounded by alternating initial segments of stable and unstable manifolds that intersect only in their endpoints. In order to fix the value of the resonance area, choose an intersection of initial segments that minimizes the area. In fig. 1 we show the fixed point resonance zone, R, for the standard map at k = 2. The boundary of R is formed by initial segments of stable and unstable manifolds of the saddle points *p* =(-0.5, 0) and *q* = (0.5, 0). These segments also intersect at the heteroclinic points a and b.

When 0<k<4 the central feature of the resonance is the elliptic island that is centered at the elliptic fixed point e with coordinates (0,0). For larger k this fixed point is unstable (hyperbolic with reflection);however, since *p* and *q* are still hyperbolic the resonance can still be constructed.

More generally a resonance is constructed from periodic orbits with frequency m/n. For the case of a twist mapping on the cylinder Aubry-Mather theory [16,17] implies that for every ω there exist special orbits called minimizing orbits; these are generically hyperbolic. Let $\{x_t\}$ denote a minimizing orbit with frequency(m,n). These orbits are ordered in the sense that for two points x_t, $x_{t'}$ on the orbit and any $j \in \mathbb{Z}$,

$$x_t < x_{t'} + j$$

This implies, in particular, that the points x_t lie on the circle in the same order as the points mt/n. Furthermore the orbit can be organized into an orbit of gaps—let x_{t+r} be the nearest point to the right of x_t on the minimizing orbit; then the gap g_t is defined as

$$g_t = \{x:$$

By the ordering condition, one can consider the mapping to act on the gaps, $f(g_t) \equiv g_{t+1}$. If the minimizing orbit is unique, then the set of its gaps covers the circle.

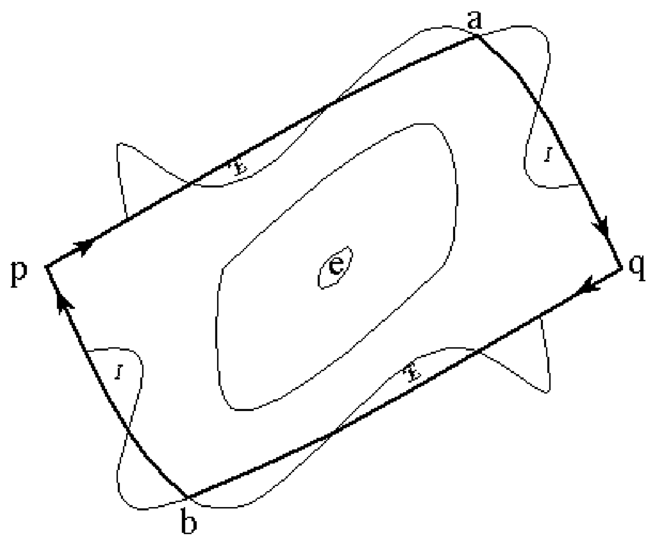

Fig. 1 Resonance for the standard map at k = 2.0. The resonance boundary is the thick curve, the points *p* and *q* are the hyperbolic fixed points, *e* is the elliptic fixed point and *a* and *b* are heteroclinic points. The exit set consists of the two regions labeled $\mathcal{E}$, and the entry set of the two labeled *I*. The upper and lower turnstiles consist of the entry sets together with the preimages of the entry sets (what one might call the incoming sets). Two invariant curves from the family that encloses the elliptic fixed point are also shown.

Associated with each minimizing periodic orbit, there are minimizing homoclinic orbits, $x_t^{\pm}$, that live in the gaps of the minimizing orbit, $x_t^{\pm} \in g_t$. The *right-going* homoclinic x_t^{+} is forward asymptotic to the orbit of the right endpoint of the gap and backward asymptotic to its left endpoint; similarly x_t^{-} labels the *left-going* homoclinic. Switching back to x-y coordinates, we can use these orbits to construct the boundary of the resonance, by choosing some point on the right-going homoclinic orbit to switch from unstable to stable manifold forming the upper resonance boundary and similarly a point on the left-going homoclinic orbit to form the lower resonance boundary.

Any orbit that remains forever inside a resonance has the same rotation frequency as the resonance.

One may imagine coloring points in the resonance zone according to their exit or transit times. In this case the color would change only upon crossing a stable or unstable manifold of the hyperbolic periodic orbit. The reason is that discontinuities of the exit time occur only at points whose forward orbits intersect the boundary of the resonance zone. Since the boundary is composed of segments of stable and unstable manifolds, the orbits of discontinuity points in the interior of the zone must land on a segment of stable manifold in the exit set.

There are several difficulties with the computation of this decomposition. First one has to construct the resonance zone and its exit and entry sets, and then the algorithm has to decide whether a point is contained within some preimage of the exit set or not—a computation that becomes increasingly difficult as the preimages become folded and stretched. Furthermore and most importantly, the construction of resonance zones and their exit sets cannot be carried out for higher dimensions, at least not in terms of the stable and unstable manifolds of a periodic orbit since these have at most half the dimension of the phase space for a symplectic map.

5. Escape from the Strip

Nonetheless, we would like to group orbits that have similar behavior together. One such grouping is in terms of the rotation frequency vector of an orbit, if it exists: orbits with the same frequency can be viewed as similar.

Consider for the moment the two dimensional case, and the set of orbits that do not rotate—those with rotation frequency zero. More simply consider the orbits whose x coordinate remains in the interval [-0.5,0.5], the gap between the hyperbolic fixed points. Thus we compute the exit time decomposition of the vertical strip

$$V = \{(x,y): -.5 \; {}^{2} \; x \; {}^{2} \; .5\}. \qquad (10)$$

The exit and entry sets for V, which overlap, are easily obtained analytically for any particular mapping. For example, in the case of the standard map the exit set is

$$\mathcal{E}_1 = \left\{(x,y) : y > 0.5 - x + \frac{k}{2\pi}\sin(2\pi x), \text{ or } \; y < -0.5 - x + \frac{k}{2\pi}\sin(2\pi x)\right\} \text{ab} \; (11)$$

while the entry set is

$$\mathcal{I}_1 = \{(x,y) : y > 0.5 + x, \text{ or } \; y < -0.5 + x\} \qquad (12)$$

These are sketched in Fig. 2 for the standard map. Note that the fixed point resonance is approximately outlined after a single iteration. In general, for a twist map, the vertical boundaries of V map to curves that are the graphs over the x-axis, and therefore the region that does not exit in one iterate forward or backward is compact.

Let U denote the set of all points in the x-y plane whose orbits are contained in V. It is clear that the invariant set U is contained in the white region of Fig. 2 and therefore is compact. It has a complicated fractal structure because of the heteroclinic cycle associated with the fixed point resonance.

Numerical computations for some finite number of iterations give an indication of the structure of U. In Fig. 3 we show the exit time decomposition of V. Note that the discontinuities in the colors become increasingly similar to the stable manifolds of the fixed points. Figure 4 shows the transit time decomposition; here the discontinuities are caused by curves that approximate both stable and unstable manifolds. The black regions contain U; it consists of a large connected component surrounding *e* as well as disconnected islands. In the figures one can see black islands corresponding to a period 7 oscillating island chain. Since only 32 iterations have been done, a number of features are not seen; for example, there is a pair of period five islands embedded in the connected chaotic component of the resonance zone. These are within the connected black component of the figures; however, exit time computations for larger times also outline these features.

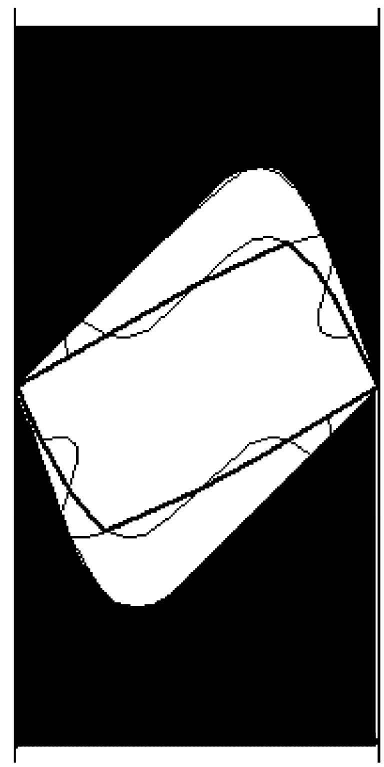

Fig. 2 Exit and entry sets for the vertical strip when k = 2. The dark region is in both $\mathcal{E}$ and I, and thus has a transit time of2.

Fig. 3.Exit time decomposition of the strip V for k = 2. The domain of the figure is (-0.5,0.5)×(-1.0,1.0). Escape times 1,2,3,4,5,...} correspond to the colors {red, green, blue, yellow, light blue, ...}. Black points stay in for at least 32 iterates (SEE NOTE AT THE END OF THE PAPER REGARDING COLORFIGURES).

Fig. 4 Transit time decomposition of the strip V for k = 2. The map was iterated 32 times forward and backward. Red corresponds to a transit time of 2, with the colors incremented as in Fig 3. The dust of light blue points correspond to those with transit times of 61--63.

The escape time distribution, e_t, the fraction of trajectories escaping per unit time, is shown in Fig 5 for several parameter values. The distribution appears to decay as $t^{-\alpha}$, thought it is difficult to determine α over the computation time. Similar computations of the distribution(called the “trapping statistics”) using the quadratic mapping for10^8 iterates gave $\alpha \approx 2.5$ [18], and for the 10^7 iterates of the standard map $\alpha \approx 2.45$ [19,20] (here the distribution of “Poincaré recurrences” was computed; this is proportional to the integral of the escape time distribution).

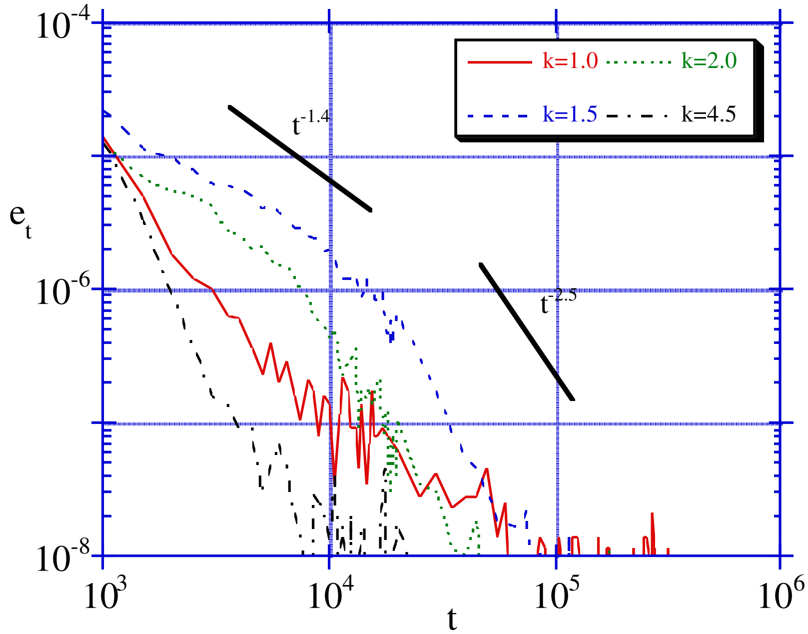

Fig. 5Escape Time distribution for the standard map using the width function—see §6. The calculations were done on a 500×500pixel grid on the domain (–.5,.5)×(–1,1), except for k = 4.5 which used a 700×700 grid. The distribution is the relative measure escaping per unit time for those particles that do eventually escape. The large fluctuations when e_t is small are statistical in nature.

We can show that the maximal invariant set inside the resonance zone is equal to the maximal invariant set in the strip V. Thus the set of points that have long exit times from the strip approximates the maximal invariant set in the resonance zone.

Hypothesis A: Let f be a twist map of the plane with a hyperbolic fixed points *p* and *q*. We assume there is a choice of initial segments of the stable, W^s, and unstable, W^u,manifolds of *p* and *q* such that a resonance zone can be constructed within the vertical strip V= $\{(x,y)$: $\pi(p)\ ^2\ x\ ^2\ \pi(q)\}$ (see Fig. 6).Here, π denotes the projection onto the x-axis. Let *a* and *b* designate the right- and left-going heteroclinic points at which the switch from W^u to W^s occurs, respectively, and let v_a and v_b denote the vertical lines through *a* and *b*, respectively. We further assume that the upper resonance boundary intersects v_a only at *a*, and the lower resonance boundary intersects v_b only at *b*.

These assumptions are verified numerically for the standard map. They can also be proved to hold for the mapping (3) when the potential v(x) is bimodal and when k is large enough. In this case there is a choice of homoclinic point for which the resonance boundaries are Lipschitz graphs [21]; this is sufficient for the validity of hypothesis A.

Under these assumptions we have the result:

> **Theorem1:** For a twist map satisfying hypothesis A, the maximal invariant subset of V is contained in the resonance R.

We begin the proof with a simpler proposition. Denote the vertical line through q by v_q, and choose another vertical line ℓ to the left of q, see Fig 7. Let S denote the open strip between ℓ and v_q. We denote by $W^s[c,d)$ the half open segment of the right-going stable manifold of q between points c and d. The point of $\ell \cap W^s$ closest to q along W^s is denoted a. Thus the open segment of stable manifold $W^s(a,q)$ is contained in S. By the Jordon curve theorem, the set S-$W^s(a,q)$ is the disjoint union of two open connected sets T and B, with T "above" B.

> **Proposition2:** Every point in the closure of T that does not belong to $W^s[a,q]$ exits (to the right) from the closure of S.

Proof: We begin by showing that $f(T) \cap S$ is contained in a subset of T. Let ℓ_1 be the leftmost vertical line intersected by $W^s[f(a), q)$. Note that ℓ_1 is contained in S because $W^s[f(a),q) \subset S$. Define S_1 to be the open strip between the lines ℓ_1 and v_q.

Define a_1 to be the point on $\ell_1 \cap W^s[f(a), q)$ that is closest to q along W^s. Thus $W^s(a_1, q)$ is contained in S_1. By the Jordon curve theorem, the set S_1-$W^s(a_1, q)$ is the disjoint union of two open connected sets T_1 and B_1, with T_1 above B_1.

Since f twists to the right, the image of every vertical is a graph over the x-axis. Thus there exists a point $b \subset \ell$ above a such that $f(b) \subset v_q$. Denote the vertical line segment joining a and b by γ. Furthermore $f(b)$ must be above q, since otherwise $f(\gamma)$ would intersect $W^s(f(a),q)$,which it cannot do since γ does not intersect $W^s(a,q)$. Let δ be the vertical line segment joining q and $f(b)$.

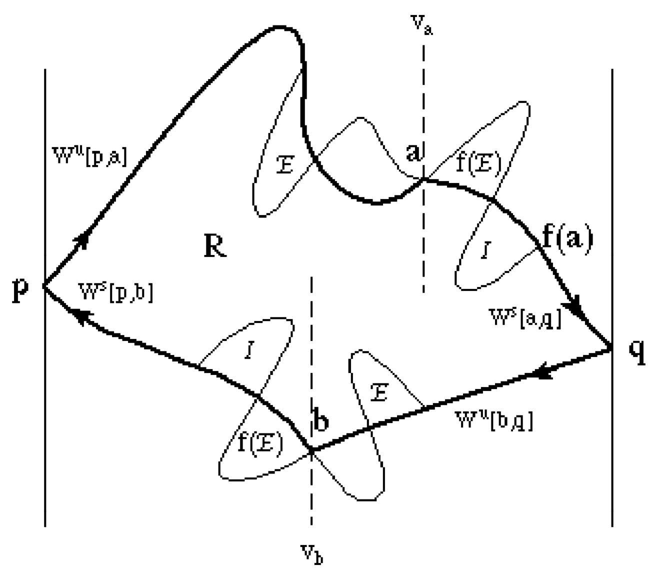

Fig.6 Assumptions on the geometry of the resonance, R. For hypothesis A, R must be contained in the strip between p and q, and the verticals through the heteroclinic points a and b intersect the upper and lower boundaries, respectively, at only one point. For hypothesis B, each turnstile and and its iterate must be separated by the verticals through a and b, respectively.

Then $f(T) \cap S$ is a bounded open set with boundary equal to the simple closed curve consisting of the three arcs $f(\gamma)$,$W^s[f(a),q]$, and δ. Thus by the Jordon curve theorem, $f(T) \cap S$ is connected. Furthermore, $f(T) \cap S$ is contained in S_1 because its boundary is contained in the closure of S_1. Finally, $f(T) \cap S$ is contained in either T_1 or B_1 because it is connected and does not intersect $W^s[a_1, q]$. However, since the closure of $f(T) \cap S$ contains the point $f(b)$, $f(T) \cap S$ must be contained in T_1.

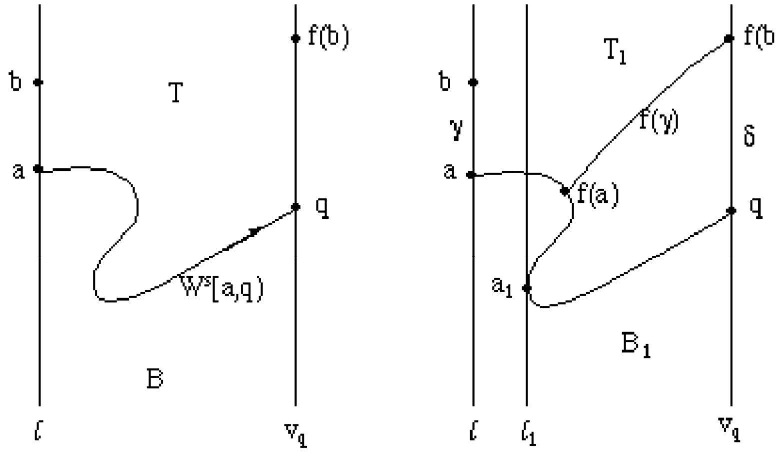

Fig.7. Definition of the regions T, B, T_1 and B_1 for the proof of Proposition 2.

Repeat the preceding arguments on S_1 constructing a sequence of strips S_j and points a_j. The points a_j converge to q at least as fast as the iterates of a. Therefore the lines ℓ_j converge to the line v_q. Further, if we assume that the orbit of a point z is contained in T then $f^j(z)$ belongs to T_j.

Thus if the orbit of z does not exit from S, then its omega limit set would have to be contained in δ. However, since f has twist, the only invariant set in δ is q. Thus z must belong to the stable manifold of q. However, by assumption every point in T and hence z is not in $W^s[a,q]$. Therefore for some j>0, $f^j(z)$ belongs to the half open segment $W^s[a, f(a))$ of stable manifold between a and f(a). This segment is outside the closure of f(T)∩S and hence $f^j(z)$ does not belong to this closed set. This is a contradiction because $f^j(z)$ does belong to f(T)∩S . Hence the orbit of z must exit from S.

By twist, every point on the vertical half lines above b and q maps outside the closure of S. The vertical segment γ between a and b maps into T. Thus every point in the closure of T that does not belong to $W^s[a,q]$ exits to the right from the closure of S. ❑

In the proof of Prop. 2 we did not assume that the segment of stable manifold $W^s(f(a),q)$ is contained in the strip between v_q and $v_{f(a)}$; however, Prop. 2 actually implies that this is true and thus that $a_1 = a$. This follows since every point in T_1must exit S, so T_1 cannot intersect $W^s[a,q]$. Applying the same conclusion to the original strip S shows that the preimage of $W^s[a,q]$ cannot intersect T.

Proof of theorem 1: The complement of the resonance zone can be broken into four pieces. Each piece is the part of a vertical strip above or below a segment of stable or unstable manifold forming the boundary of the resonance zone. For example, one piece is the part of the strip between the vertical lines v_a and v_q that is above the stable segment $W^s[a,q]$. By Prop. 2 the forward orbits of all points in this piece exit this strip to the right. A second piece of the complement is the part of the vertical strip between the lines v_p and v_a that is above the unstable segment W^u[p,a]. Proposition 2 applied to f^{-1}, which is a left-twisting map, shows that the backward orbit of any point in this piece exits this strip to the left. The two pieces of the complement that are below the resonance zone are treated similarly. ❑

For an (m,n) resonance, the strip V is replaced by a set of n strips using the gaps in the minimizing periodic orbit. Let V_t be the vertical strip defined by the closure of the gap g_t associated with a minimizing (m.n) orbit: $V_t = \{z : \pi(z) \in \overline{g}_t\}$.Then an orbit is said to be in the set of strips V_t if there is a k∈Z such

$$\pi(z_t) \in \overline{g}_{t+k} \text{ for all } t\in Z \tag{13}$$

Since the stable and unstable manifolds of the minimizing orbit and its right neighbor intersect to form a heteroclinic cycle, the resonance construction can be generalized to this case [5] and is easy to generalize Th. 1:

> **Theorem 3**:For a twist map satisfying hypothesis A for the (m,n) resonance, the set of points whose orbits are contained in the sequence of strips V_t associated with the (m,n) resonance is identical to the maximal invariant set of the (m,n) resonance.

Thus the invariant sets contained in the strips are identical to those in the resonance zones. Furthermore a result of Easton implies that the asymptotic escape rates for these sets are the same, since they can be made into nested isolating blocks [22]. It is numerically simpler to construct the exit time decomposition for the strip than for the resonance itself. However, our prime motivation for this construction is its generalization to four dimensions, which we defer until §7.

One deficiency of the strip is that it uses vertical lines as boundaries. These appear artificially since they have no invariant definition—though of course the vertical is privileged due to the definition of twist. We discuss an alternate definition next.

6. The Width Function

For a symplectic twist map, f, of the plane, the *width* of a point z=(x,y) relative to frequency ω is defined as

$$w_\omega(z) = \sup_t \left[\pi\left(f^t(z)\right) - \omega t\right] - \inf_t \left[\pi\left(f^t(z)\right) - \omega t\right] \tag{14}$$

where t is any integer. The set of points with $w_\omega \le 1$ will be denoted $\mathcal{W}_\omega$. This set is invariant, since according to the definition $w_\omega(z) = w_\omega(f(z))$. If the width of an orbit is bounded, then the orbit $\{z_t\}$ has rotation number ω, according to the definition (4).

A similar set is $\mathcal{L}_\omega$, which denotes the set of points whose orbits remain close to the linear orbit

$$\mathcal{L}_\omega = \left\{z : \left|\pi\left(f^t(z)\right) - z - \omega t\right| \le 1\right\}. \tag{15}$$

This is an interesting set, since there is an ω such that each ordered orbit,(8), is in $\mathcal{L}_\omega$ [3]. In particular the minimizing and minimax orbits of frequency ω are in $\mathcal{L}_\omega$. We can show that $\mathcal{W}_\omega$ is a subset of $\mathcal{L}_\omega$; moreover,

> **Lemma 4**: $\mathcal{W}_\omega$ is the maximal invariant subset of $\mathcal{L}_\omega$.

Proof: First we show that $\mathcal{W}_\omega \subset \mathcal{L}_\omega$;for if $z \in \mathcal{W}_\omega$, then, letting $x_t = {}^1(f^t(z))$, we have

$$-1 \le [x_{t+j} - \omega(t+j)] - [x_t - \omega t] \le 1$$

for any t and j, since otherwise the width would be too large. Rearranging this gives $|x_{t+j} - x_t - \omega j| < 1$, and thus $z_t \in \mathcal{L}_\omega$. Furthermore, if there is a point $z \in \mathcal{L}_\omega$ whose orbit is also in $\mathcal{L}_\omega$, then we have $| x_{t+j} - x_j - \omega t | \leq 1$ for any t and j, so

$$| x_{t+j} - \omega(j+t) - (x_j - \omega j) | \leq 1$$

which implies that $w_\omega(z_j) \leq 1$.❑

We will now show that the set of orbits of width one is also contained within the resonance, and therefore computations of the width function can be used to describe exit times. We begin by considering the(0,1) resonance, setting $\omega = 0/1$, and dropping the subscript, $\mathcal{W} = \mathcal{W}_0$.

Hypothesis B: We assume in addition to hypothesis A, that the upper turnstile is entirely to the left of the vertical line v_a, and that its iterate is entirely to the right of v_a. Consequently the upper entry set $\mathcal{E}$ is entirely to the left of v_a and the upper exit set $\mathcal{I}$ is entirely to the right of v_a, recall Fig. 6. We make a similar assumption about the lower turnstile, relative to the line v_b.

This hypothesis appears true for the standard map from numerical computations. For the case considered by Veerman and Tangerman [21], the boundaries of the turnstile can be chosen to be Lipschitz graphs, and so the turnstile is contained in a vertical strip, and the exit set and the preimage of the entry set are separated by a vertical line. This, while not quite equivalent to hypothesis B, is also sufficient to prove the next theorem.

> **Theorem 5:**For a twist map satisfying hypothesis B, the set of orbits $\mathcal{W}$ is the maximal invariant set in the (0,1) resonance R (or more precisely the set of integer translates of R).

We begin the proof with a simpler proposition. Denote the vertical line through q by v_q, and choose another vertical line r to the right of q. Let S′ denote the open strip between v_q and r. Let W^u denote the right-going unstable manifold of q. The point of $r \cap W^u$ closest to q along $W^u$is denoted a'. Thus the open segment of unstable manifold $W^u(q,a')$ is contained in S′. By the Jordon curve the theorem, the set S′-$W^u(q,a')$ is the disjoint union of two open connected sets T′ and B′, with T′ "above" B′.

> **Proposition6:** Every point in the closure of T′, except q, either exits to the right from the closure of S′ or enters B′.

Proof: The inverse of f is also a twist map that twists to the left. Therefore the closure C of $f^{-1}(T')\cap T'$ is a compact set. By the twist condition, the boundary of the set T′-C maps to the right of r or into B′, thus each point of the closure of T′ not in C exits S′ to the right, or enters B′. On the other hand, suppose z belongs to C. If the orbit of z does not enter B′ and does not exit from S′ then it must remain in C. Thus its omega limit set, $\Omega(z)$, is anon-empty invariant set. Note that $\Omega(z)$ is not contained in $W^u[q,a']$ because if it were then $\Omega(z)$ would have to be the fixed point q. In this case some iterate of z would belong to the local stable manifold of q; however, the local stable manifold of q does not intersect C, because, for a right twist map, the right going branch of the local unstable manifold is above the right going branch of the local stable manifold (as is easy to demonstrate by looking at the matrix Df(q)). Therefore there exists a point w in $\Omega(z)$ that is not in $W^u[q,a']$. However in this case, according to Prop. 2 for f^{-1}

applied to the strip S′, the backward orbit of *w* must exit the strip to the left. This contradicts the invariance of $\Omega(z)$.❑

Proposition7: Consider the union of the two strips S and S′. Let z belong to the closure of T∪T′ minus $W^s[a,q]$ and $W^u[q,a']$. If the orbit of z does not intersect B or B′ then it must cross S∪S′ from left to right.

Proof: Suppose first that z belongs to the closure of T minus $W^s[a,q]$. By Prop. 2, the orbit of z exits the strip S to the right. Since by hypothesis it cannot enter B′ it must enter T′ or exit S∪S′ to the right as required. On the other hand, if it enters T′ or starts in the closure of T′ then Prop 6 implies that it must also exit S′ to the right. Finally, to show that the backward orbit must exit to the left, apply the preceding argument to f^{-1}.❑

Proof of Theorem 5: The upper boundary of the resonance R and its translates form a “partial barrier” separating the plane into top and bottom components. If an orbit stays above R and its translates, then Prop. 7 implies that the orbit has width greater than 1. Orbits that cross the partial barrier must intersect the sets $\mathcal{E}$ or $\mathcal{I}$ or their translates. Consider an orbit that crosses from below through the set $\mathcal{E}$. If it recrosses the barrier then some point on the orbit must be in $\mathcal{I}$ or one of its translates. By hypothesis B the distance between $\mathcal{E}$ and each of the translates of $\mathcal{I}$ is greater than one, so in this case the width would be greater than one. On the other hand, an orbit that intersects $\mathcal{E}$ cannot re-enter the resonance through $\mathcal{I}$, because by hypothesis B, the image of $\mathcal{E}$ is to the right of the vertical line that forms the right boundary of T, and every point in T exits to the right by Prop. 2.

A similar argument works for orbits that start below the chain of translates of R. Thus the only orbits of width less than or equal to 1 must be contained in one of the translates of R. ❑

The generalization of the theorem to an (m,n) resonance that satisfies hypothesis B is straightforward. It is based on the fact that such a resonance has a turnstile in only one of the n islands, and thus when a point is above the resonance, it is forced to rotate around the cylinder at least m times before it could possibly enter the resonance.

We show computations of the exit times using the width criterion in Figs. 9 and 10. One advantage of the width criterion, over the strip, is that there is no artificial discontinuity on vertical lines—the discontinuity appearing with the choice w = 1 is dynamically significant since this corresponds to the orbit undergoing a complete rotation around the cylinder. Secondly, one does not have to know the position of the hyperbolic periodic points in order to compute the width. Otherwise Fig. 9 is quite similar to Fig. 4. The discontinuities appear to lie along approximations of the stable and unstable manifolds. Another advantage of the width function is that it allows classification of the trapped orbits. In the figures we color those orbits with w < 1 for the first 100 iterates according to their widths—this shows the structure of the trapped invariant set. Figure

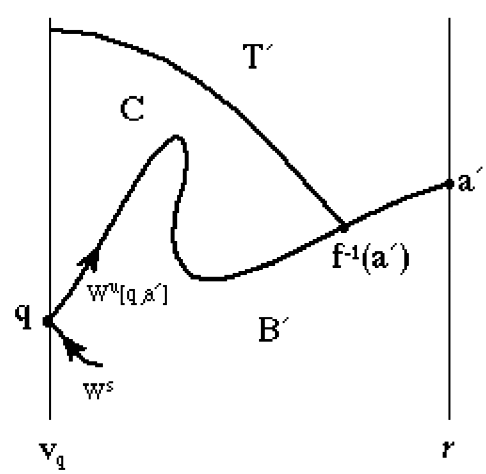

Fig. 8. Sketch for the proof of Proposition 6.

10 displays a computation for the case when the fixed point at x = 0 has become unstable to a period two orbit. The light blue curves outline the stable and unstable manifolds in a striking way.

As k increases, the computations give a nice visualization of the formation of the horseshoe in the resonance zone R; this occurs slightly below k =8.3. The exit time decomposition in the case of the horseshoe corresponds simply to the cantor set construction of the horseshoe itself.

Fig. 9.Transit times computed for the standard map at k = 2.0 using the width function; boundaries are the same as Fig. 3. The colors ranging from black through orange to yellow then white correspond to orbits whose width exceeds one during its first 100 iterates. Orbits with w<1 are colored green to magenta to blue in the direction of decreasing width. These correspond to the orbits trapped in the resonance.

Fig. 10. Transit times for k = 4.7 using the width function; boundaries are the same as Fig. 3. Colors ranging from light to dark blue to yellow correspond to the time at which the width exceeds one, up to 100 iterates. Orbits with w<1 are colored shades of red.

7. Four Dimensions

Little is known about transport in high dimensional phase spaces. Numerical studies indicate that some structure analogous to resonances appears to exist [23]. Some results were obtained by Wiggins [11], who studied a weakly coupled pair of area preserving maps, one of which is integrable and the other of which has a transverse homoclinic connection. In this case, stability of normally hyperbolic sets implies that the standard two dimensional transport results persist for weak coupling.

Here we consider an example introduced by Froeschlé [24]corresponding to coupled standard maps The family on $T^2 \times R^2$ is given by (5) with the potential

$$v(x_1, x_2) = \frac{-1}{4\pi^2}\{a \cos(2\pi x_1) + b \cos(2\pi x_2) + c \cos[2\pi(x_1+x_2)]\} \tag{16}$$

There are(generically) four fixed points at $(x,y) = (^1/_2(m,n),\ 0)$, where $m,n \in \{0,1\}$—these correspond to critical points of v. Typically one of these points is hyperbolic, one elliptic, and two are half elliptic and half hyperbolic(i.e. one eigenvalue pair of unit modulus and the other real). For small c and positive a and b, are four hyperbolic fixed points in C located at (-.5,-.5,0,0), (.5,-.5,0,0),(-.5,.5,0,0), and (.5,.5,0,0). The point with coordinates (0,0,0,0) is elliptic.

An analogue of the strip considered before is the "cylinder"

$$C = \{(x,y) \in R^4 : |x_1| \le 0.5, |x_2| \le 0.5\}; \tag{17}$$

this set is quite natural when c = 0. We study the maximal invariant set in C in terms of the exit time function.

The stable and unstable manifolds of the hyperbolic fixed points are two dimensional and therefore do not separate volumes in phase space. It is no longer possible to construct a resonance zone whose boundary consists of pieces of stable and unstable manifolds of hyperbolic fixed points. However, it does make sense to study the maximal invariant set contained in C. The geometry of this set may reveal how Arnold diffusion occurs in the neighborhood of the elliptic fixed point (0,0,0,0).

The invariant set contained in C is compact, a fact that follows from

Proposition8: The set $C \cap f^{-1}(C)$ is diffeomorphic to a four dimensional cube.

Proof: Let $\varphi: R^4 \to R^4$ be the smooth map defined by

$$\varphi(x,y) = (x,{}^1(f(x,y)) = (x,x') \ .$$

Since f is a twist map, φ restricted to the set ${}^{1\text{-}1}(x)$ is one to one, and the set $\{{}^1(f(x,y)) : y \in R^2\}$ is the entire plane. It follows that φ is one to one and onto. The Jacobian matrix of φ has the form

$$D\varphi = \begin{pmatrix} I & 0 \\ \frac{\bullet x'}{\bullet x} & \frac{\bullet x'}{\bullet y} \end{pmatrix}$$

By the twist condition, the 2 by 2 submatrix _x′/_y is non-singular; therefore $D\varphi$ is non-singular. Hence by the inverse function theorem, φ has a smooth inverse and is therefore a diffeomorphism. From the definition of φ it follows that the set $C \cap f^{-1}(C)$ is mapped to the four dimensional cube

$$K = \left\{ \{(x,x') \in R^4 : |x_j| \le 0.5, |x'_j| \le 0.5, \text{ for } j = 1,2 \right\} \ .❏$$

It follows immediately from Proposition 8 that the maximal invariant set contained in C is compact. The geometry of this invariant set can be probed by taking two dimensional slices of C and restricting the exit time function to these slices. The intersection of the invariant set with such a slice is the set of points with infinite forward and backward exit times. Pixels are colored as before according to exit time from C. The curves that separate regions of different colors are evidently generated by the intersections of preimages of the three dimensional boundary of C with the chosen two dimensional plane slice of C. This is reasonable because a three dimensional submanifold intersects a two dimensional submanifold of a four dimensional manifold generically in a one dimensional manifold or curve.

For the four dimensional case, the width of an orbit can be computed in any direction in the configuration space. For lack of a compelling choice, we take the width to be the maximum of the widths computed for each component; in other words, for $z = (x_1,x_2,y_1,y_2)$ we compute the widths

$$w_1(z) = \sup_t (x_{1t}) - \inf_t (x_{1t}) \ ; \quad w_2(z) = \sup_t (x_{2t}) - \inf_t (x_{2t}) \tag{18}$$

and define

$$w(z) = \max(w_1(z),w_2(z)) \quad . \tag{19}$$

Thus an orbit can acquire large width either by rotating in the x_1 or the x_2 direction.

As a corollary to Prop. 8, the set of orbits in $T^2 \times R^2$ for which $w \le 1$ is also compact, since it is contained in the set for which

$$\max(|x_1 - x_1'|, |x_2 - x_2'|) \le 1.$$

There are a number of interesting two dimensional slices; in Fig 11 we show four. The top two panels are the canonical planes and since the complementary canonical pair is set to zero, the exit time distribution appears similar to two dimensional case; however, in detail the shapes are unlike the structure of the standard map pictures—note particularly the red regions in the left panel. The bottom left panel shows the momentum plane for $\mathbf{x} = \mathbf{0}$. It shows a connected trapped(black) region surrounding $\mathbf{y} = \mathbf{0}$ that is the analogue of the island surrounding the fixed point in the two dimensional case. Most orbits within this region lie on invariant two-tori. It appears that this region is a four-volume. Note however the appearance of escaping (white and red)regions within the connected black component—these can never occur in the two dimensional case. The last panel shows the configuration plane for $\mathbf{y} = \mathbf{0}$; since the domain of the figure is$(-1,1)\times(-1,1)$ there are nine copies of the elliptic point shown. Note that the boundary between fundamental domains on T^2 is complex implying that we should use a different norm than that in (19).

The orbits trapped near the elliptic fixed point are outlined even with short time computations of the width function, as shown in Fig. 12 for the $\mathbf{x} = \mathbf{0}$ slice. Here the first 100 iterates are colored using the scale shown. Those orbits that escape in times 100 to 10^6 are shown in white, and those whose exit time is larger than 10^6 are black. The set of trapped orbits becomes increasingly well defined for long times and there are disconnected components (corresponding to islands around the main island) and holes as before. Nevertheless, most orbits escape in the first 100 iterations, and by 10^6 iterations, as far at the computations are concerned, almost no orbits escape.

Fig. 11.Exit times using the width function for the Froeshlé map with a = 1.0, b= 2.0, and c = 0.8. Each panel represents a different slice: the planes$(x_2,y_2) = \mathbf{0}$, $(x_1,y_1) = \mathbf{0}$, $(x_1,x_2) = \mathbf{0}$, and $(y_1,y_2) = \mathbf{0}$.The domain of each panel is $(-1,1)\times(-1,1)$. Colors range from blues for short times, to reds for intermediate times, to greys for longer times. Points that do not escape in 100 iterates are colored black.

Fig. 12. Exit times using the width function for the slice $\mathbf{x} = \mathbf{0}$ for the Froeshlé map with a = 1.0, b = 0.5 and c = 1.0. The domain of the figure is $(y_1,y_2) = (-0.5,0.5)\times(-0.5,0.5)$. The colors ranging from blue to white indicate exit times between 1 and 100 as shown in the color scale at the bottom. Points that have $w<1$ for 10^6 iterates are colored black.

The escape time distribution computed using the width function for various parameter values is shown in Fig. 13. The distribution is power law in nature, $e_t \sim t^{-\alpha}$, with an exponent that ranges from about $\alpha = -1.1$ for the case c = 0.01, to $\alpha = 1.3$ for c = 0.1. No exponents significantly deviating from these have been observed, but it is not known whether there is a universal exponent associated with this process. These exponents are considerably smaller than those observed for the two dimensional case, recall Fig. 5, though much longer computations would be required to confirm this smaller value for α.

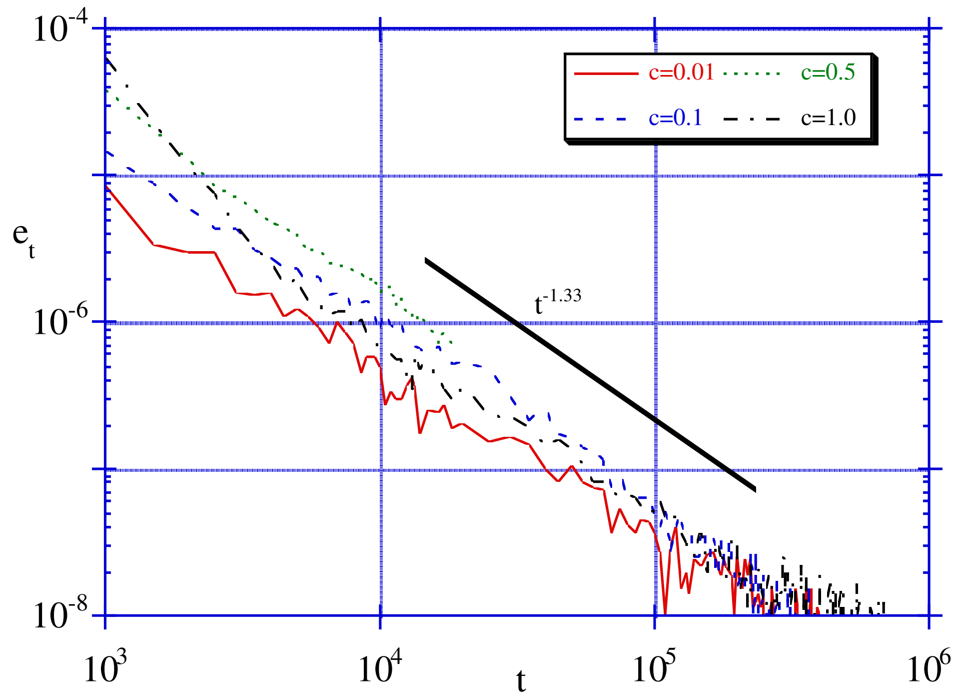

Fig 13.Normalized escape time distributions (time at which the width exceeds unity) for initial points in the **x** = **0** slice for a=1.0 and b=0.5 with varying values of c. The vertical axis is the probability of escape per unit time for those particles that do eventually escape. The computations were done for a box of size 500×500 pixels, each was iterated up to 10^6 steps. The statistics become noisy when $e_t < 2(10)^{-8}$ as only a few particles escape during each temporal bin of 5000 iterates.

Fig. 14. Enlargement of a small region in the **x** = **0** plane for a=1.0, b = 1.5, c = 0.5. The domain of the figure is (0.085,-0.24)×(0.145,-0.228). Exit times for the first 1000 iterates are shown using the width function. The color scale is shown at the bottom of the figure. Note the disconnected red regions, and the varying complexity of the border ofthe non-escaping black region.

8. Conclusions

The exit and transit time decompositions of a set yield statistical measures of transport with physical relevance. For the two dimensional case, resonance zones are the dynamically natural regions to use for these studies; however, we have shown that the set of orbits trapped a vertical strip, or set of strips, containing the resonance is identical to that of the resonance itself. Thus the exit time distribution of the resonance and the strip have the same asymptotic form. Furthermore, since the stable and unstable manifolds of the resonance need not be constructed to study escape from the strip, the computations are easier. A third measure of escape is provided by the width function, that measures the deviation of an orbit from a given frequency of rotation. For a given rational frequency, the set of orbits of width less than one is identical to those trapped in the resonance. An orbit whose width exceeds one has rotated around the cylinder at least once more or less then it should have. The calculation of the width function does not require that the hyperbolic periodic orbit be found, and thus it is easily implemented.

For four and higher dimensional systems there is no simple construction of a resonance zone. Nevertheless, computations of escape from a four dimensional cylinder as well as those of orbits with width less than one show that there are four dimensional regions trapped around an elliptic fixed point analogous to those orbits trapped in a 2D resonance. These volumes include the families of invariant tori given by the KAM theorem, but undoubtedly also include orbits that are not strictly stable, and that will eventually escape. However, the computations imply there is a zone of "practical" stability, and it is this concept that the computations quantify. The boundary of this trapped set contains smooth regions as well as disconnected tubes that appear to wend their way into the midst of the trapped regions. We do not have, as of yet, a dynamical explanation of these.

A number of other open questions remain. We do not know whether the set of orbits trapped in the cylinder C is identical to those of width less than one, as it is in the two dimensional case. Furthermore, though the choice of the strip in the two dimensional case is natural, since its boundaries are formed from vertical lines through the hyperbolic fixed points, for four dimensions only the 2 dimensional edges of the cylinder C are similarly natural—there is no dynamical reason to use 3 dimensional planes to connect these edges. Similarly it is not clear which of the translates of the hyperbolic fixed points should form the proper fundamental domain for the definition of the cylinder. A related issue arises with the proper choice of norm for the width function. In the norm we used, (19), there is an artificial use of the square in configuration space as the boundary.

Acknowledgements

Partial support for this research was obtained from the National Science Foundation through grant DMS-9001103. S. Carver was supported by an REU supplement to this grant.

References

1. Ottino, J. M., *The Kinematics of Mixing: Stretching, Chaos, and Transport*, (Cambridge Univ. Press, Cambridge, 1989).

2. Wiggins, S., *Chaotic Transport in Dynamical Systems*, Interdisciplinary Applied Mathematics, (Springer-Verlag, New York,1991).

3. Meiss, J. D., "Symplectic Maps, Variational Principles, and Transport," Rev. Mod. Phys., **64**, 795-848 (1992).

4. MacKay, R. S., J. D. Meiss and I. C. Percival, “Transport in Hamiltonian Systems,” Physica, **13D**, 55-81 (1984).

5. MacKay, R. S., J. D. Meiss and I. C. Percival, “Resonances in Area Preserving Maps,” Physica, **27D**, 1-20 (1987).

6. Easton, R. W., “Transport Through Chaos,” Nonlinearity, **4**, 583-590 (1991).

7. Rom-Kedar, V. and S. Wiggins, “Transport in Two-Dimensional Maps,” Arc. Rational Mech. Anal., **109**, 239-298 (1988).

8. Chen, Q., “Area as a Devil’s Staircase in Twist Maps,” Phys. Lett., **123A**, 444-450 (1987).

9. Hanson, J. D., J. R. Cary and J. D. Meiss, “Algebraic Decay in Self-Similar Markov Chains,” J. Stat. Phys., **39**, 327-345(1985).

10. Chen, Q. and J. D. Meiss, “Flux, Resonances and the Devil’s Staircase for the Sawtooth Map,” Nonlinearity, **2**, 347-356(1989).

11. Wiggins, S., “On the Geometry of Transport in Phase Space, I. Transport in k-Degree of Freedom Hamiltonian Systems, 2^2k<_,”Physica, **40D**, 471-501 (1990).

12. Nekhoroshev, N. N., “An Exponential Estimate for the Stability Time of Hamiltonian Systems Close to Integrable Ones,” Russ. Math. Surveys, **32:6**, 1-65 (1977).

13. Warnock, R. L. and R. D. Ruth, “Long-term bounds on nonlinear Hamitonian motion,” Physica, **56D**, 188-255 (1992).

14. MacKay, R. S., J. D. Meiss and J. Stark, “Converse KAM Theory for Symplectic Twist Maps,” Nonlinearity, **2**, 555-570 (1989).

15. Golé, C., “Monotone Maps of TN X RN and their Periodic Orbits,” J. Diff. Eq., **in press**, (1991).

16. Aubry, S., “The Twist Map, the Extended Frenkel-Kontorova Model and the Devil's Staircase,” Physica, **7D**, 240-258 (1983).

17. Mather, J. N., “Existence of Quasi-periodic Orbits for Twist Homeomorphisms of the Annulus,” Topology, **21**, 457-467 (1982).

18. Karney, C. F. F., “Long Time Correlations in the Stochastic Regime,” Physica, **8D**, 360-380 (1983).

19. Chirikov, B. V. and D. L. Shepelyansky, “Statistics of Poincaré Recurrences and the Structure of the Stochastic Layer of a Nonlinear Resonance,” Princeton Plasma Physics Laboratory Report#PPPL-TRANS-133 (1983).

20. Chirikov, B. V. and D. L. Shepelyanksy, “Correlation Properties of Dynamical Chaos in Hamiltonian Systems,” Physica, **13D**, 395-400(1984).

21. Veerman, J. J. P. and F. M. Tangerman, “Intersection Properties of Invariant Manifolds in Certain Twist Maps,” Comm. Math. Phys., **139**, 245-265 (1991).

22. Easton, “Transport of Phase Space Volume near Isolated Invariant Sets,” University of Colorado Report (1992).

23. Kook, H. T. and J. D. Meiss, “Periodic Orbits for Reversible, Symplectic Mappings,” Physica, **35D**, 65-86 (1989).

24. Froeschle, C., “Numerical Study of a Four Dimensional Mapping,” Astron. and Astrophys, **16**, 172-189 (1972).

Color Figures

We have not included copies of the color figures with this preprint, because of the cost. Should you wish to have high quality color xerox copies of these 7 figures, please send $10.00 to

James Meiss
Program in Applied Mathematics
Box 526
University of Colorado
Boulder, CO 80304